



## Purification of Planarian Stem Cells Using a Draq5-Based FACS Approach

Kuang-Tse Wang, Justin Tapper, and Carolyn E. Adler

### Abstract

Planarians are flatworms that have the remarkable ability to regenerate entirely new animals. This regenerative ability requires abundant adult stem cells called neoblasts, which are relatively small in size, sensitive to irradiation and the only proliferative cells in the animal. Despite the lack of cell surface markers, fluorescence-activated cell sorting (FACS) protocols have been developed to discriminate and isolate neoblasts, based on DNA content. Here, we describe a protocol that combines staining of far-red DNA dye Draq5, Calcein-AM and DAPI, along with a shortened processing time. This profiling strategy can be used to functionally characterize the neoblast population in pharmacologically-treated or gene knockdown animals. Highly purified neoblasts can be analyzed with downstream assays, such as in situ hybridization and RNA sequencing.

**Key words** Flatworms, Fluorescence-activated cell sorting, Regeneration

---

### 1 Introduction

Planarians have the remarkable ability to regenerate entire new animals from small pieces of tissue, making them an intriguing model to study regeneration [1, 2]. Planarian tissue turnover and regeneration are fueled by an active adult stem cell population, referred to as neoblasts. Neoblasts are the only proliferative cells in planarians and produce new cells that replenish missing and damaged tissues [3]. Therefore, characterizing neoblasts and their behavior is one of the primary goals of research in planarian biology.

Although fluorescence-activated cell sorting (FACS) commonly relies on the unique expression of cell-surface markers to selectively purify populations of cells from animals, such molecules presenting on the surface of planarian neoblasts remain largely unknown. Therefore, purification of neoblasts relies on the fact that these are the only actively dividing cells in the animal, their sensitivity to irradiation, and their relatively small size. Based on

these properties, isolation of neoblasts often combines a DNA dye together with a dead-cell dye to eliminate necrotic cells, as well as their depletion after radiation to confirm the purification strategy [4–12]. Further verification of neoblasts by morphological criteria and in situ hybridization of neoblast markers, such as *cyclin-B* and *Smedwi-2*, demonstrates that these crude markers are sufficient to isolate neoblasts with high purity from the animal [4, 13–17]. FACS also enables analysis of the dynamics of neoblasts with additional dyes, such as the apoptotic marker annexin V, following various perturbations to the animals [9, 18, 19]. FACS-sorted neoblasts have been used in downstream assays such as RNA-seq [20–26], ChIP-seq [21, 27–29], in situ hybridization [15, 30], and single-cell RNA sequencing [30–36], which facilitates the understanding of neoblast characteristics.

Although the most commonly used DNA dye for purifying neoblasts is Hoechst 33342 [4], there are limitations to its use. In particular, current gating strategies depend on the dual blue and red emissions from Hoechst 33342 following exposure to UV light. Reliance on two-color emissions precludes addition of other short wavelength and red dyes for certain experimental design strategies. Also, some instruments may not have a UV laser available. Use of alternative DNA dyes, including Sir-DNA and Draq5, both of which emit in far red, has been used for neoblast culture [33, 37] and neoblast isolation, respectively, along with verification by single-cell RNA sequencing [35, 38].

Here, we describe a detailed protocol that combines Draq5, Calcein-AM, and DAPI to isolate the mitotic neoblast population. Draq5 emission occupies the far-red spectrum, so we include DAPI to identify dead cells and Calcein-AM as a vital marker to ensure the isolation of healthy cells. Application of these three dyes is simultaneous, shortening the total processing time. More importantly, the use of this dye combination frees the red channel for incorporation of dyes in this spectrum.

---

## 2 Materials

### 2.1 *Animals for Cell Dissociation*

This protocol has been optimized with animals cultured in the lab derived from a clonal strain of *Schmidtea mediterranea* [39, 40]. Before dissociation, starve the animals for at least 1 week to eliminate food debris. To standardize cell numbers expected for each dissociation, select animals of similar sizes. We typically use ten 3–5 mm animals per sample, which yields  $\sim 2 \pm 0.5$  million live cells per mL. When conducting the experiment for the first time, generate lethally irradiated animals as a negative control to properly establish the gating strategy. Two days after radiation exposure, animals no longer have mitotic neoblasts.

**2.2 Cell Dissociation**

1. CMF: 400 mg/L NaH<sub>2</sub>PO<sub>4</sub>, 800 mg/L NaCl, 1200 mg/L KCl, 800 mg/L NaHCO<sub>3</sub>, 240 mg/L Glucose, 15 mM HEPES. To prepare 1× CMF, dissolve NaH<sub>2</sub>PO<sub>4</sub>, NaCl, KCl, NaHCO<sub>3</sub>, and Glucose in ultrapure water to the desired volume. Add HEPES buffer to 15 mM, filter-sterilize and store the solution at 4 °C for future use.
2. CMFB: CMF, 1% (w/v) BSA. On the day of cell dissociation, weigh out BSA and add to CMF to make CMFB. To dissociate and process a single sample, usually 20 mL of CMFB is more than sufficient (*see Note 1*). For example, add 0.2 g BSA to 20 mL CMF in a 50 mL conical tube and rock on a nutator to dissolve the powder. Sterilize by filtering this solution using 0.22 μm low protein binding syringe filters and keep on ice.

**2.3 Live Cell Staining**

1. Calcein-AM stock solution: 2 mM Calcein-AM in DMSO. Dissolve 50 μg Calcein-AM powder (ThermoFisher C3100MP) in 250 μL DMSO. Protect this solution from light and store at –20 °C for future use. Samples will be stained using a 4 μM working stock solution.
2. Draq5 stock solution (eBioscience/ThermoFisher 65-0880-92): 5 mM Draq5. Protect this solution from light and store at 4 °C for future use. Samples will be stained using a 10 μM working stock solution.
3. DAPI stock solution: 5 mg/mL DAPI in water. Add 2 mL ultrapure water to 10 mg DAPI powder (ThermoFisher 62247). Protect this solution from light and store at 4 °C for future use. Samples will be stained using a 5 μg/mL working stock solution.
4. Trypan Blue solution (VWR 76180-676): Store this solution at room temperature.

**2.4 Common Equipment**

1. SonyMA900 FACS sorter.
2. Sorvall Legend XIR centrifuge (or equivalent swinging bucket refrigerated centrifuge).
3. 0.22 μm low protein binding syringe filters (Millex SLGV004SL).
4. TC20 Automated Cell Counter (Bio-Rad 1450102).
5. TC20 Cell counting slides (Bio-Rad 1450015).
6. 30 μm Filcon filters (BD Biosciences 340627).
7. Thermo Scientific Multi-tube rotator (or equivalent nutator).
8. MicroScalpel (VWR 100491-038) (or equivalent blade for cutting animals).
9. 35 mm Petri dish (VWR 82050-536).
10. Transfer pipette (VWR 14670-149).
11. 5 mL tubes (LPS L225001).

---

### 3 Methods

#### 3.1 Cell Suspension Preparation

1. Keep the CMFB at 4 °C or on ice (*see Note 2*).
2. Place ten animals into a 35 mm plastic dish.
3. Remove the planarian water from the animals and replace with ~3 mL CMFB.
4. Using a sharp scalpel, cut all animals into tiny fragments, ensuring that all fragments should be less than ~1 mm in size (*see Note 3*).
5. Collect the fragments with a transfer pipette and move them into a 5 mL tube. Transfer them quickly to prevent fragments from sticking to the inside of the transfer pipette (*see Note 4*).
6. Cool the centrifuge to 4 °C. Every 5 min, triturate the worms using a P1000 pipette and allow the sample to rock on the nutator for 20 total minutes (*see Note 5*). As the dissociation progresses, the solution should become opaque and lack pigmented fragments (*see Note 6*).
7. Once the fragments are sufficiently dissociated, pass the suspended cells through a 30 µm Filcon filter into a new 5 mL tube.
8. Spin the tubes at  $500 \times g$  for 5 min at 4 °C. A dark pellet should appear after centrifugation.
9. Aspirate the supernatant carefully, leaving the pellet in a small amount of liquid so that it does not fully dry out. Gently resuspend the pellet in 2 mL CMFB using a P1000 pipette.

#### 3.2 Cell Counting

1. Mix 10 µL of the cell suspension from the filtered samples with 10 µL Trypan Blue solution (in a 1.5 mL Eppendorf tube). Then load 10 µL of the dye mixture into a hemocytometer slide (*see Note 7*).
2. Count cells using a hemocytometer or TC20 Automated Cell Counter. This protocol should provide  $\sim 2 \pm 0.5$  million live cells per mL (*see Note 8*). Using a centrifuge, spin at  $500 \times g$  for 5 min at 4 °C. A dark pellet should be visible after centrifugation. Store the samples on ice while preparing staining solutions or proceed to the next step immediately.

#### 3.3 Cell Staining

1. Thaw the Calcein-AM stock solution in the dark.
2. Calculate the desired volume of dye solution. We typically stain cells at a final concentration of 2 million cells per mL. For example, make 2 mL of dye solution to stain 4 million cells (*see Note 9*).
3. Make the dye solution by diluting 1:500 Calcein-AM stock solution, 1:500 Draq5 stock solution and/or 1:1000 DAPI stock solution (*see Note 10*). For example, to make 10 mL of

dye solution, add 20  $\mu\text{L}$  Calcein-AM stock solution, 20  $\mu\text{L}$  Draq5 stock solution and 10  $\mu\text{L}$  DAPI stock solution. Invert the dye solution several times to ensure mixing. Once mixed, protect the solution from light.

4. Resuspend the cell pellet in the appropriate volume of dye solution and place the tubes on a nutator at room temperature for 20 min in the dark.
5. Once the staining is completed, wrap the tubes with foil and keep on ice.

### 3.4 Cell Sorting

1. Immediately before sorting, refilter the cells into a new tube using a fresh 30  $\mu\text{m}$  Filcon filter (*see Note 11*).
2. Set up the lasers and cool down the FACS machine to 4  $^{\circ}\text{C}$  if possible. Load the tubes into the FACS machine and sort your samples (*see Note 12*). We use the 100  $\mu\text{m}$  nozzle for sorting. The gating strategy for isolating the mitotic neoblast population is described in Subheading 3.5.

### 3.5 Gating the Mitotic Neoblast Population

1. Eliminate cell aggregates by using forward scatter (FSC) and side scatter (SSC). Outliers with bigger sizes and high morphological complexity can be cell aggregates, which will show high DNA content in downstream gates and distort the analysis (Fig. 1a, b) (*see Note 13*).
2. Gate for DAPI-negative and Calcein-AM-positive cells to enrich for live cells. Only dead cells are permeable to DAPI, while vital cells can absorb Calcein-AM and convert it to a fluorescent form. Use the FITC filter to record Calcein-AM emission (as in Fig. 1c) (*see Note 14*).
3. Identify Draq5-positive cells, which are nucleated, in APC versus 750 nm filter using linear scales. The APC and 750 filter together can record the far-red emission of Draq5 (Fig. 1d).
4. Set up Calcein-AM versus APC-A gates. The 4N (DNA content) cells represent the mitotic neoblast population (X-ray-sensitive cell fraction-1: X1), and have higher than average APC intensity. Mitotic cells are sensitive to irradiation, so they should be absent in the irradiated sample (X1 in Fig. 1e, f).
5. The post-mitotic progeny of neoblasts (X-ray-sensitive cell fraction-2: X2) are 2N and also irradiation-sensitive (X2 in Fig. 1e, f). The remainder of the cells represent the 2N differentiated cell population (X-ray-insensitive cell fraction: Xins) (Xins in Fig. 1e, f).
6. Collect the sorted cells into an Eppendorf tube containing 50  $\mu\text{L}$  CMFB.
7. Centrifuge your collected cells at  $500 \times g$  for 5 min at 4  $^{\circ}\text{C}$ . A dark blue pellet may be visible (*see Note 15*).

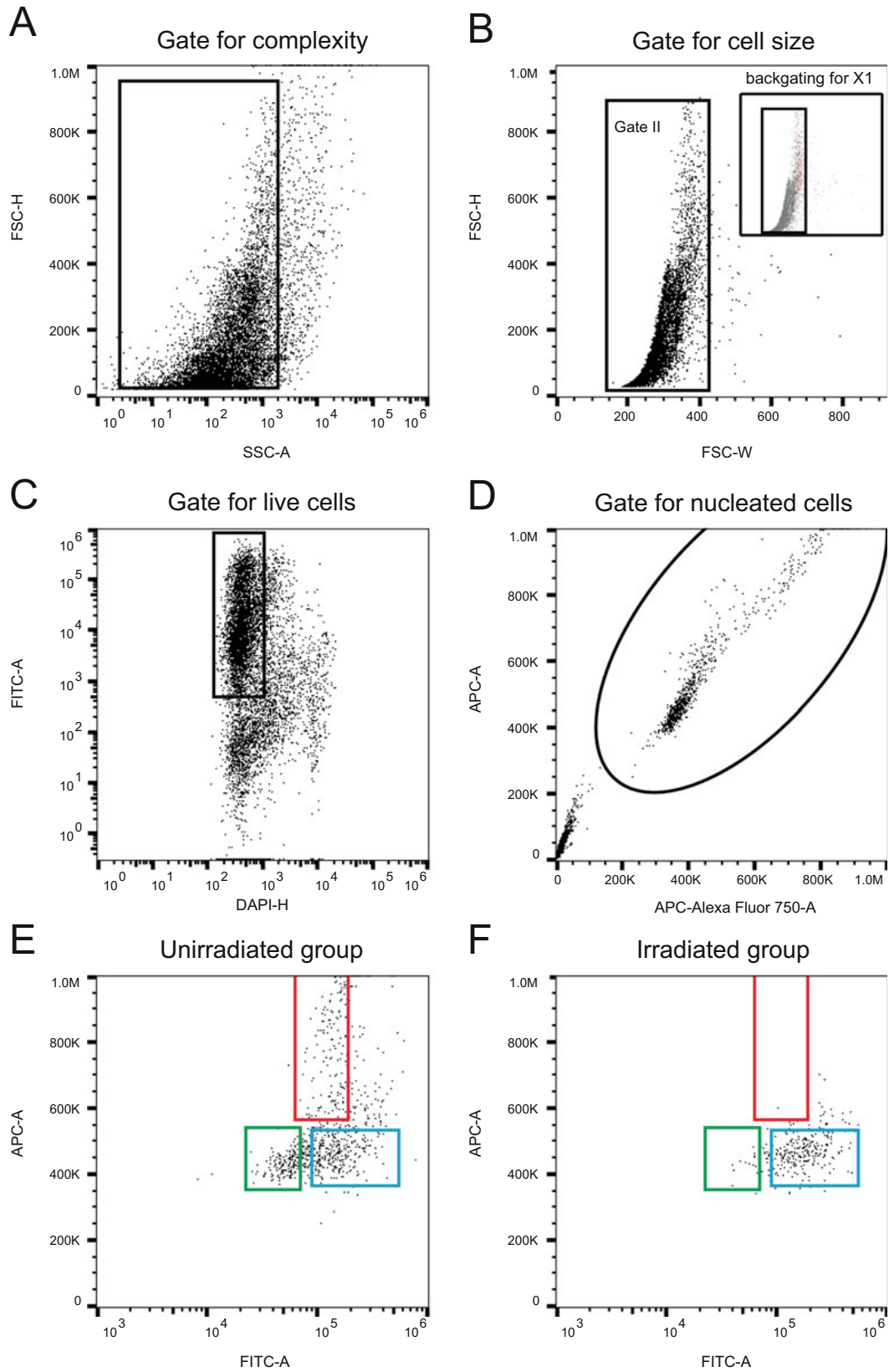


**Fig. 1** FACS gating strategy for neoblasts. The heading of each panel indicates the objectives of the gating strategy. The order of the panels follows the hierarchy of the gating. (a) Dot plot showing side scatter area

8. Carefully aspirate the supernatant and resuspend the cells in 100  $\mu$ L CMFB.
9. Count cells using a hemocytometer or TC20 Automated Cell Counter (*see Note 16*).
10. Centrifuge your collected cells at  $500 \times g$  for 5 min at 4  $^{\circ}$ C, and resuspend the cells into the desired buffer at the appropriate density for downstream applications.
11. The sorted cells may now be used for imaging, in situ hybridizations, or sequencing.

---

#### 4 Notes

1. Do not vortex CMFB. Vortexing will generate bubbles which may complicate downstream volume measurements.
2. To increase cell viability for downstream applications, maintain cells at 4  $^{\circ}$ C as much as possible.
3. Cutting fragments to a size of  $\sim 1$  mm or smaller will accelerate dissociation of the fragments. Larger or heterogeneously-sized fragments will slow down dissociation, requiring more processing and handling, ultimately decreasing the overall health of the dissociated cells. Enzymatic dissociation methodologies, including papain and liberase treatments have also been used to accelerate dissociation without harming mitotic neoblasts [9, 41–43].
4. If fragments adhere to the inside of the transfer pipette, dislodge them by vigorously pipetting CMFB up and down and flicking the pipette near where the fragment is stuck.
5. For trituration, use a P1000 set to 500  $\mu$ L and rapidly pipette up and down. This is particularly important at the beginning, to initiate dissociation. In the first several triturations, some fragments will inevitably adhere to the inside of the tip. Due to

---

**Fig. 1** (continued) (SSC-A) versus forward scatter height (FSC-H). FSC intensity increases in proportion to cell size, and side scatter detects cellular complexity. We eliminate the SSC outliers to reduce cell aggregates, which tend to have higher complexity. **(b)** Dot plot showing forward scatter width (FSC-W) versus forward scatter height (FSC-H). For further eliminating cell aggregates, we gate for cells with mild forward scatter width. Inset, backgating of D. Red dots are cells in the X1 gate, which lies close to the right boundary of Gate II. **(c)** Dot plot showing DAPI-height (DAPI-H) versus FITC-area (FITC-A). The Calcein-AM is detected by the FITC filter. Live cells will be DAPI-negative and Calcein-AM positive. **(d)** Dot plot showing Alexa Fluor 750 nm area (APC-Alexa Fluor 750-A) versus APC-A (APC-area). Draq5 is excited by the 633 nm laser, and its emission is detected through APC ( $>650$  nm) and far red (750 nm) filters. **(e, f)** Dot plots of cells in Gate IV showing the FITC-A versus APC-A in unirradiated and irradiated animals, respectively. X1 cells (red) are defined as the mitotic, 4N neoblast population. X2 cells (green) are the post-mitotic progeny of neoblasts. Radiation depletes the X1 and X2 populations **(f)**, but not the radiation-insensitive differentiated cells (Xins, blue)

the time-sensitive nature of this step, simply discard the pipette tip and prepare for the next trituration to maximize efficient dissociation.

6. Mechanical force will dissociate all planarian tissues with the exception of the animal's pharynx. Towards the end of the dissociation, these pharynges will become apparent as small white objects. The rest of the solution will appear opaque.
7. Our lab uses a TC20 Automated Cell Counter to count cells and determine the percentage of live and dead cells with trypan blue staining. However, the cell counter can overestimate cell numbers. As a result, we strongly recommend optimizing the cell counting method in each lab to ensure reliability. Calculate the cell number by multiplying the cell counts by the dilution factor, which is 2 in this example because the cell suspension is diluted 1:1.
8. Live cells typically represent 50–60% of the total population of dissociated cells.
9. For consistent dye staining across samples, it is necessary to adjust the volume of staining solution with cell density. Otherwise, cells may be oversaturated or have inconsistent staining, leading to variability in cell sorting across experiments. Prior to sorting, the final cell concentration should be adjusted according to instrument specifications.
10. When performing this method for the first time, allocate some cell suspension for staining with single dyes. These single-stained samples are used for setting up fluorescent compensation on the flow cytometer. Fluorescent compensation corrects fluorescence spillover when the emission spectrum of each dye overlaps with other dyes.
11. This additional 30  $\mu\text{m}$  filtration removes clumps of cells, reducing the probability of clogging the FACS machine.
12. The size of the collection tube may vary depending upon the downstream application or the specific FACS machine used.
13. The mitotic neoblast population lies on the right boundary of Gate II (Fig. B inset, red dots). Therefore, if the XI population cannot be found, shift the boundary of Gate II rightward.
14. Dye-negative cells can be determined by comparing profiles of single-stained samples.
15. In some cases, especially if fewer than  $\sim 20,000$  cells were sorted, pellets may not be visible after centrifugation.
16. To conserve as many cells as possible for downstream applications, dilute the cells 1:10 with Trypan Blue solution. It is also possible to use a standard trypan blue staining as described in Sect. 3.2.

## References

1. Rink JC (2018) Stem cells, patterning and regeneration in planarians: self-organization at the organismal scale. *Methods Mol Biol* 1774:57–172
2. Reddien PW (2018) The cellular and molecular basis for planarian regeneration. *Cell* 175:327–345
3. Rink JC (2013) Stem cell systems and regeneration in planaria. *Dev Genes Evol* 223:67–84
4. Hayashi T, Asami M, Higuchi S, Shibata N, Agata K (2006) Isolation of planarian X-ray-sensitive stem cells by fluorescence-activated cell sorting. *Develop Growth Differ* 48:371–380
5. Romero BT, Evans DJ, Aboobaker AA (2012) FACS analysis of the planarian stem cell compartment as a tool to understand regenerative mechanisms. *Methods Mol Biol* 916:167–179
6. Hayashi T, Agata K (2018) A subtractive FACS method for isolation of planarian stem cells and neural cells. *Methods Mol Biol* 1774:467–478
7. Mohamed Haroon M, Lakshmanan V, Sarkar SR, Lei K, Vemula PK, Palakodeti D (2021) Mitochondrial state determines functionally divergent stem cell population in planaria. *Stem Cell Rep* 16:1302–1316
8. Molinaro AM, Lindsay-Mosher N, Pearson BJ (2021) Identification of TOR-responsive slow-cycling neoblasts in planarians. *EMBO Rep* 22:e50292
9. Shiroor DA, Bohr TE, Adler CE (2020) Injury delays stem cell apoptosis after radiation in planarians. *Curr Biol* 30:2166–2174.e3
10. Kang H, Sánchez Alvarado A (2009) Flow cytometry methods for the study of cell-cycle parameters of planarian stem cells. *Dev Dyn* 238:1111–1117
11. Eisenhoffer GT, Kang H, Sánchez Alvarado A (2008) Molecular analysis of stem cells and their descendants during cell turnover and regeneration in the planarian *Schmidtea mediterranea*. *Cell Stem Cell* 3:327–339
12. Solana J, Kao D, Mihaylova Y, Jaber-Hijazi F, Malla S, Wilson R, Aboobaker A (2012) Defining the molecular profile of planarian pluripotent stem cells using a combinatorial RNAseq, RNA interference and irradiation approach. *Genome Biol* 13:R19
13. Reddien PW, Oviedo NJ, Jennings JR, Jenkin JC, Sánchez Alvarado A (2005) SMEDWI-2 is a PIWI-like protein that regulates planarian stem cells. *Science* 310:1327–1330
14. van Wolfswinkel JC, Wagner DE, Reddien PW (2014) Single-cell analysis reveals functionally distinct classes within the planarian stem cell compartment. *Cell Stem Cell* 15:326–339
15. Scimone ML, Kravarik KM, Lapan SW, Reddien PW (2014) Neoblast specialization in regeneration of the planarian *Schmidtea mediterranea*. *Stem Cell Rep* 3:339–352
16. Wagner DE, Wang IE, Reddien PW (2011) Clonogenic neoblasts are pluripotent adult stem cells that underlie planarian regeneration. *Science* 332:811–816
17. Zeng A, Li H, Guo L, Gao X, McKinney S, Wang Y, Yu Z, Park J, Semerad C, Ross E (2018) Prospectively isolated tetraspanin+ neoblasts are adult pluripotent stem cells underlying planaria regeneration. *Cell* 173:1593–1608.e20
18. Peiris TH, García-Ojeda ME, Oviedo NJ (2016) Alternative flow cytometry strategies to analyze stem cells and cell death in planarians. *Regeneration (Oxf)* 3:123–135
19. Peiris TH, Ramirez D, Barghouth PG, Ofoha U, Davidian D, Weckerle F, Oviedo NJ (2016) Regional signals in the planarian body guide stem cell fate in the presence of genomic instability. *Development* 143:1697–1709
20. Labbé RM, Irimia M, Currie KW, Lin A, Zhu SJ, Brown DDR, Ross EJ, Voisin V, Bader GD, Blencowe BJ et al (2012) A comparative transcriptomic analysis reveals conserved features of stem cell pluripotency in planarians and mammals. *Stem Cells* 30:1734–1745
21. Duncan EM, Chitsazan AD, Seidel CW, Sánchez Alvarado A (2015) Set1 and MLL1/2 target distinct sets of functionally different genomic loci *in vivo*. *Cell Rep* 13:2741–2755
22. Wenemoser D, Lapan SW, Wilkinson AW, Bell GW, Reddien PW (2012) A molecular wound response program associated with regeneration initiation in planarians. *Genes Dev* 26:988–1002
23. Vázquez-Doorman C, Petersen CP (2014) zic-1 Expression in planarian Neoblasts after injury controls anterior pole regeneration. *PLoS Genet* 10:e1004452
24. Zhu SJ, Hallows SE, Currie KW, Xu C, Pearson BJ (2015) A mex3 homolog is required for differentiation during planarian stem cell lineage development. *eLife* 4:e07025. Available at: <https://doi.org/10.7554/eLife.07025>
25. Onal P, Grün D, Adamidi C, Rybak A, Solana J, Mastrobuoni G, Wang Y, Rahn H-P, Chen W, Kempa S et al (2012) Gene expression of pluripotency determinants is conserved between mammalian and planarian stem cells. *EMBO J* 31:2755–2769

26. Sasidharan V, Lu Y-C, Bansal D, Dasari P, Poduval D, Seshasayee A, Resch AM, Graveley BR, Palakodeti D (2013) Identification of neoblast- and regeneration-specific miRNAs in the planarian *Schmidtea mediterranea*. *RNA* 19: 1394–1404
27. Dattani A, Kao D, Mihaylova Y, Abnave P, Hughes S, Lai A, Sahu S, Aboobaker AA (2018) Epigenetic analyses of planarian stem cells demonstrate conservation of bivalent histone modifications in animal stem cells. *Genome Res* 28:1543–1554
28. Mihaylova Y, Abnave P, Kao D, Hughes S, Lai A, Jaber-Hijazi F, Kosaka N, Aboobaker AA (2018) Conservation of epigenetic regulation by the MLL3/4 tumour suppressor in planarian pluripotent stem cells. *Nat Commun* 9:3633
29. Verma P, Waterbury CKM, Duncan EM (2021) Set1 targets genes with essential identity and tumor-suppressing functions in planarian stem cells. *Genes* 12:1182. Available at: <https://doi.org/10.3390/genes12081182>
30. Raz AA, Wurtzel O, Reddien PW (2021) Planarian stem cells specify fate yet retain potency during the cell cycle. *Cell Stem Cell* 28:1307. Available at: <https://doi.org/10.1016/j.stem.2021.03.021>
31. Fincher CT, Wurtzel O, de Hoog T, Kravarik KM, Reddien PW (2018) Cell type transcriptome atlas for the planarian *Schmidtea mediterranea*. *Science* 360:eaq1736
32. Plass M, Solana J, Wolf FA, Ayoub S, Misios A, Glažar P, Obermayer B, Theis FJ, Kocks C, Rajewsky N (2018) Cell type atlas and lineage tree of a whole complex animal by single-cell transcriptomics. *Science* 360:eaq1723
33. Niu K, Xu H, Xiong YZ, Zhao Y, Gao C, Seidel CW, Pan X, Ying Y, Lei K (2021) Canonical and early lineage-specific stem cell types identified in planarian SirNeoblasts. *Cell Regen* 10: 15
34. Wurtzel O, Oderberg IM, Reddien PW (2017) Planarian epidermal stem cells respond to positional cues to promote cell-type diversity. *Dev Cell* 40:491–504
35. García-Castro H, Kenny NJ, Iglesias M, Alvarez-Campos P, Mason V, Elek A, Schönauer A, Sleight VA, Neiro J, Aboobaker A et al (2021) ACME dissociation: a versatile cell fixation-dissociation method for single-cell transcriptomics. *Genome Biol* 22:89
36. Wurtzel O, Cote LE, Poirier A, Satija R, Regev A, Reddien PW (2015) A generic and cell-type-specific wound response precedes regeneration in planarians. *Dev Cell* 35:632–645
37. Lei K, Zhang W, Chen J, McKinney SA, Ross EJ, Lee HC, Sánchez Alvarado A (2023) Pluripotency retention and exogenous mRNA introduction in planarian stem cells in culture. *iScience* 26(2):106001
38. Wang K, Adler CE (2023) CRISPR/Cas9-based depletion of 16S ribosomal RNA improves library complexity of single-cell RNA-sequencing in planarians. *BMC Genomics* 24:625
39. Merryman MS, Sánchez Alvarado A, Jenkin JC (2018) Culturing planarians in the laboratory. *Methods Mol Biol* 1774:241–258
40. Newmark PA, Sánchez Alvarado A (2022) *Schmidtea* happens: Re-establishing the planarian as a model for studying the mechanisms of regeneration. *Curr Top Dev Biol* 147:307–344
41. Moritz S, Stöckle F, Ortmeier C, Schmitz H, Rodríguez-Esteban G, Key G, Gentile L (2012) Heterogeneity of planarian stem cells in the S/G2/M phase. *Int J Dev Biol* 56:117–125
42. Fincher CT, Wurtzel O, de Hoog T, Kravarik KM, Reddien PW (2018) Cell type transcriptome atlas for the planarian *Schmidtea mediterranea*. *Science* 360(6391):eaq1736
43. Shiroor DA, Wang K, Sanketi BD, Tapper JK, Adler CE (2023) Inhibition of ATM kinase rescues planarian regeneration after lethal radiation. *EMBO reports* 24:e56112